

*Carnegie Observatories Astrophysics Series, Vol. 3:
Clusters of Galaxies: Probes of Cosmological Structure and Galaxy Evolution
ed. J. S. Mulchaey, A. Dressler, and A. Oemler (Cambridge: Cambridge Univ. Press)*

The Formation of Early-Type Galaxies: Observations to $z \sim 1$

T. TREU

California Institute of Technology, Astronomy 105-24, Pasadena, CA, 91115, USA

Abstract

How does the number density of early-type galaxies (E+S0) evolve with redshift? What are their star formation histories? Do their mass density profile and other structural properties evolve with redshift? Answering these questions is key to understanding how E+S0s form and evolve. I review the observational evidence on these issues, focusing on the redshift range $z \sim 0.1 - 1$, and compare it to the predictions of current models of galaxy formation.

1.1 Introduction

Understanding the formation and evolution of early-type galaxies (E+S0, i.e. ellipticals and lenticulars) is not only crucial to unveil the origin of the Hubble sequence, but is also a focal point connecting several unanswered major astrophysical questions. The hypothesis that E+S0s form by mergers of disks at relatively recent times is one of the pillars of the cold dark matter (CDM) hierarchical scenario. At galactic scales, since they are the most massive galaxies, E+S0s are the key to understanding how and when dark and luminous mass are assembled in galaxies, and to test the universal form and ubiquity of dark matter halos predicted by the CDM paradigm (Navarro, Frenk & White 1997, hereafter NFW; Moore et al. 1998). On subgalactic scales, the existence of a correlation between black-hole mass and spheroid velocity dispersion suggests that the growth of black holes and the activity cycles in active galactic nuclei are somehow intimately connected with the formation of spheroids. Therefore, a unified formation scenario must ultimately be conceived (e. g. Kauffmann & Haehnelt 2000; Monaco, Salucci & Danese 2000; Volonteri, Haardt & Madau 2003; see also the proceedings of meeting I of the Carnegie Observatories Centennial).

Theoretical formation scenarios are often grouped into two categories, broadly referred to as the *monolithic collapse* and *hierarchical formation**.

In the traditional picture – the monolithic collapse – E+S0s assembled their mass and formed their stars in a rapid event, of much shorter duration than their average age (Eggen, Lynden-Bell & Sandage 1962; Larson 1975; van Albada 1982). The formation process happened at high redshifts and proto early-type galaxies would be star forming and dust-enshrouded systems. These kinds of models are consistent with a variety of features (see

* A complete review of the theoretical background is beyond the aims of this observational review. For more information the reader is referred to, e.g., the reviews by de Zeeuw & Franx (1991), Bertin & Stiavelli (1993), Merritt (1999), Peebles (2002), de Freitas Pacheco, Michard & Mohayaee (2003), and references therein.

T. Treu

Matteucci 2002 and references therein) including the homogeneity of the present day stellar populations (Sandage & Visvanathan 1978), the existence of metallicity gradients (Sandage 1972) and the characteristic $R^{1/4}$ surface brightness profile (de Vaucouleurs 1948).

By contrast, in the “hierarchical scenario” – hereafter the *standard model* – early-type galaxies form by mergers of disks at relatively recent times (Toomre & Toomre 1972; Toomre 1977; White & Rees 1978; Blumenthal et al. 1984). The formation process is continuous: mass is accreted over time, and both major and minor mergers can induce star formation thus rejuvenating at times the stellar populations. Furthermore, environmental processes – such as galaxy interactions – can be built into the models and predictions made of the properties of E+S0s as a function of environment (Kauffmann 1996; Benson, Ellis & Menanteau 2002). Examples that can be tested against observations include the global properties of E+S0s, such as the color-magnitude relation or the age of the integrated stellar populations. Increasingly sophisticated numerical cosmological simulations are being developed: it has recently become possible to simulate in detail* the formation of individual E+S0s in a fully cosmological context (Meza et al. 2003). This opens up the possibility of using observations of the internal structure (e.g. the mass density profile) of E+S0s as a test of the *standard model*.

A common and practical tool are the so-called pure luminosity evolution (PLE) models. In these phenomenological models, E+S0s form at a given redshift of formation (z_f) and evolve only through the evolution of their stellar populations. Typically, the star formation history is assumed independent of present day luminosity. For a given star formation history, stellar evolution models, and present day luminosity function, it is straightforward to compute observable properties, such as number counts and observed color distribution. PLE models are often used as toy-realizations of the monolithic collapse models and their predictions contrasted to the *standard model* predictions. However, it should be kept in mind that PLE models are only a phenomenological tool, not coincident with monolithic collapse.

For decades, the only way to test and improve our understanding of the formation process was through observations of the local universe. The only accessible pieces of information were observables such as color or spectra of local E+S0s.

This has dramatically changed in the last few years. The sharp images taken by the Hubble Space Telescope (HST), together with the high-quality ground based data collected by large aperture telescopes equipped with modern instruments, have opened up the cosmic-time domain. Now E+S0s can be identified, counted, and studied as a function of redshift (i.e. cosmic time) out to look-back times that are a significant fraction of the lifetime of the Universe. Increasingly detailed information (luminosity, color, redshift, internal kinematics, mass estimates from dynamics and lensing) for distant E+S0s can now be obtained, allowing for increasingly stringent tests of the cosmological model.

Clearly, the combination of both pieces of information – local and high redshift data – is what delivers the most stringent observational tests. Since other speakers at this meeting have covered the local Universe (e.g. Davies), I will focus specifically on the study of distant E+S0s. In particular, I will cover the redshift range $0.1 < z < 1$, corresponding in the currently favored Λ CDM cosmology† to look-back times of 1 to 8 Gyrs, thus approximately

* Note however that crucial mechanisms such as star formation can only be treated in a simplified way by means of semi-analytical recipes.

† I assume the Hubble Constant to be $H_0 = 65h_{65} \text{ km s}^{-1} \text{ Mpc}^{-1} = 100h \text{ km s}^{-1} \text{ Mpc}^{-1}$, $h_{65} = 1$ when needed. The matter density and cosmological constant in critical units are $\Omega_m = 0.3$ and $\Omega_\Lambda = 0.7$, respectively.

T. Treu

the second half of the life of the Universe. I will discuss E+S0s in general, irrespective of their environment. When needed, I will distinguish between field and cluster E+S0s to contrast different evolutionary histories. A final caveat is that I will mostly consider the broad class of spheroids (E+S0), without distinguishing between pure ellipticals and lenticulars. This simplification should be kept in mind when interpreting observational results, given that Es and S0s might have significantly different formation histories (e.g., Dressler et al. 1997; Trager 2003). When possible I will discuss the results in terms of pure Es or S0s.

I will concentrate on three key questions:

- (1) How does the number density of E+S0s evolve with time?
- (2) What is the star formation history of E+S0s?
- (3) What is the distribution of mass in E+S0s and how does it evolve with time?

In the next sections, I will review observational work on each of these questions, discuss comparison with model predictions and briefly comment on future perspective.

1.2 Evolution of the number density

How many E+S0s are there at any given redshift? Ideally, in order to compare directly with models of structure formation, we would like observations to deliver the volume density of E+S0s as a function of mass and redshift. The closest available observable to the mass function is the luminosity function $\phi(L, z)$. If luminosity evolution is understood, $\phi(L, z)$ can be used to derive the evolution of the number density at a fixed present day equivalent luminosity.

Before we proceed, it is useful to introduce a simple parametrization of $\phi(L, z)$ that can be used to express observational results in a synthetic form. Assuming pure luminosity evolution and indicating stellar mass with M_* , we can express luminosity evolution as $\log L(z) = \log L(0) - [d(\log M_*/L)/dz]z$ to first order in z . Similarly, assuming that the shape of the LF is time invariant, the evolution of the overall normalization ϕ_* can be parameterized as $\phi_*(z) = \phi_*(0)(1+z)^p$.

1.2.1 The Luminosity Function of E+S0 galaxies at $z < 1$

Before considering distant galaxies, let us briefly summarize our knowledge of the local LF of E+S0s. To this aim, a compilation is shown in Figure 1.1 (heavy lines; see caption for details and references). The compilation includes LF in various photometric bands, from the blue to the near infrared. For ease of comparison, the best fit Schechter (1976) LFs have been transformed to an intermediate wavelength, using the average colors of E+S0s[‡] to obtain L_* in the I band. Note that a simple shift in color is only an approximate transformation, because of the existence of the color magnitude relation and of different definitions of magnitudes, photometric system, and morphological classes adopted by various authors (see, e.g., Kochanek, Keeton & McLeod 2001). The agreement among the most recent determinations is rather encouraging. Nevertheless, as we will see, the uncertainty in the local LF (the fossil evidence) contributes significantly to the error budget in the measurement of $\phi(L, z)$.

The most extensive study of the evolution of the luminosity function of morphologically selected early-type galaxies is based on the 145 E+S0s with $16.5 < I < 22$ in the Groth

[‡] B-I=2.1, r'-I=0.24 Fugukita, Shimasaku & Ickikawa (1995); Bz-I=2.4 Im et al. (1996); I-K=2.1 from Bower, Lucey & Ellis (1992) and Fugukita et al. (1995)

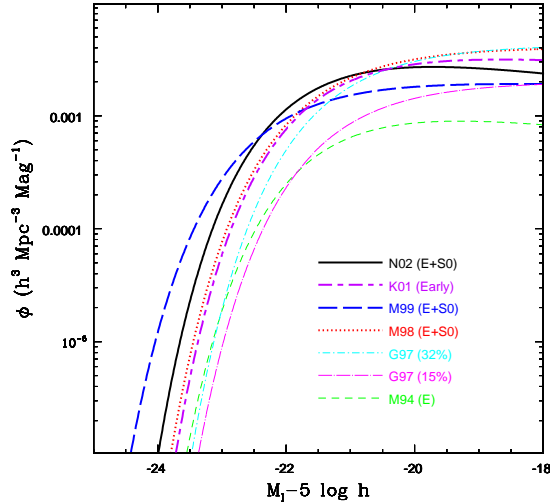


Fig. 1.1. Local luminosity functions of E+S0s transformed to the I-band, see references for details (N03=Nakamura et al. 2003, K01=Kochanek et al. 2001; M99=Marinoni et al. 1999; M98=Marzke et al. 1998). Other local LF adopted to construct PLE models are shown for comparison as thin lines (G97=Gardner et al. 1997 total K-band luminosity function scaled by 0.32 and 0.15; M94=Marzke et al. 1994 pure ellipticals luminosity function).

Strip Survey (Im et al. 2002, hereafter I02; other samples are given in Franceschini et al. 1998; Schade et al. 1999; Benson et al. 2002; given the morphological definition adopted here I will not review similar studies based on spectral classification, e.g. Cohen 2002; Willis et al. 2002). The authors use HST photometry, together with spectroscopic (45/145) and photometric redshifts (100/145), to compute the rest-frame B band luminosity, and then proceed to measure the evolution of the LF.

Based on their sample of 145 objects in the redshift range 0.1-1.2 (median redshift 0.6), I02 find $d(\log M_*/L_B)/dz = -0.76 \pm 0.32$ (i.e. 1.89 ± 0.81 mags of brightening to $z = 1$) and $p = -0.86 \pm 0.68$ (i.e. the number density at $z = 1$ is $0.55^{+0.33}_{-0.21}$ the local value). The large uncertainties arise mostly from the limited size of the sample, but also from the fact that an apparent magnitude limited sample probes different volumes and absolute magnitude ranges in the local and distant universe. Therefore bright E+S0s, dominant at large z , will have very few counter parts in the local universe and, viceversa, the faint galaxies dominating the counts in the local universe will go undetected at large z . I02 try to remove this source of uncertainty, by fixing the characteristic luminosity of the local luminosity function to some external measurement based on a larger volume. Unfortunately, I02 find very different results according to the local LF they adopt. The Marzke et al. (1998) LF yields $d(\log M_*/L_B)/dz = -0.79 \pm 0.09$ $p = -0.95 \pm 0.48$ while the Marinoni et al. (1999) LF yields $d(\log M_*/L_B)/dz = -0.41 \pm 0.09$ $p = 0.12 \pm 0.54$ (the two LF are shown in Figure 1.1 labeled as M98 and M99 respectively). In conclusion, systematic uncertainties in the local LF hinder substantial progress.

T. Treu

>From these results it is clear that a two-pronged strategy must be followed in order to improve on the current factor of 3 uncertainty in the number density evolution to $z \sim 1$. On the one hand, it is necessary to increase the size of the high redshift sample possibly to several thousands objects with a larger fraction of spectroscopic redshifts. Also a sample collected along multiple independent line of sight will be desirable to minimize the effects of cosmic variance and clustering of E+S0s (see discussion in I02 and in 1.2.2). The future prospects appear promising, due to the recent improvements of observational capabilities both on the imaging side with the Advanced Camera for Survey on HST, and on the spectroscopic side with the new generation of wide field high multiplexing spectrographs. On the other hand, it is necessary to reduce the uncertainty on the local LF of E+S0s. As illustrated in Figure 1.2 prospects look good and hopefully the optical luminosity function per morphological type will be known with higher accuracy once the morphological classification of large numbers of galaxies in the Sloan Digitized Sky Survey (SDSS) and 2dF is completed.

1.2.2 *Extremely Red Objects and the luminosity function of E+S0s at $z \sim 1$*

Old stellar populations are characterized by a sharp break in their spectral energy distribution around 4000 Å, with larger flux at longer wavelengths. Hence, an old stellar population at $z \sim 1$ appears as an object with extremely red optical to infrared colors, i.e. and Extremely Red Object (ERO). Therefore, a census of EROs would provide directly the number density of *old* E+S0s at $z \gtrsim 1$ without the need for spectroscopic redshifts, provided contaminants such as cold stars or dust enshrouded galaxies could be removed.

Several optical-infrared surveys over the past five years have been conducted with the goal of measuring the number density evolution of E+S0s (Zepf 1997; Moustakas et al. 1997; Barger et al. 1999; Benitez et al. 1999; Menanteau et al. 1999; Treu & Stiavelli 1999; Thompson et al. 1999; Daddi et al. 2000a,b; McCracken et al. 2000; Yan et al. 2000; Corbin et al. 2000; Martini 2001; McCarthy et al. 2001; Firth et al. 2002; Chen et al. 2002; Smith et al. 2002; Roche et al. 2002). A selection of the results is shown in Figure 1.2. In spite of the slightly different color cuts adopted by various groups, it is clear that those surveys conducted over sufficiently wide areas and/or along multiple lines of sight (where clustering bias and cosmic variance are unimportant) are in good agreement.

A comparison with the local abundance of E+S0s can be done considering simple PLE models. Given a spectral evolution model and the selection criteria of an ERO survey, we can obtain the set of redshifts $\mathcal{Z}(L)$ at which a galaxy of present day luminosity L would be included in the sample (typically an interval limited on the low redshift side by the red color criterion and on the high redshift side by the detection limit). Then, the density of EROs is obtained by integrating the local luminosity function times the cosmic volume per unit solid angle dV/dz over the appropriate range in luminosity and redshift:

$$\int_{L_{\min}}^{L_{\max}} \int_{\mathcal{Z}(L)} \phi(L) \frac{dV}{dz} dz dL. \quad (1.1)$$

For a local Schechter luminosity function with a flat faint end slope (c.f. Fig 1.1), the model number density depends linearly on the local characteristic density, while the dependence on the characteristic luminosity is a rapidly varying function of the depth of the survey. At L_* – where the LF is steep – an uncertainty of 0.3(0.5) mags in the assumed L_* affects the predicted counts at the 50%(80%) level. At $L_*/10$ the same uncertainties affect the counts only at the 10% (20%) level. The same calculation can be used to estimate the effects of the

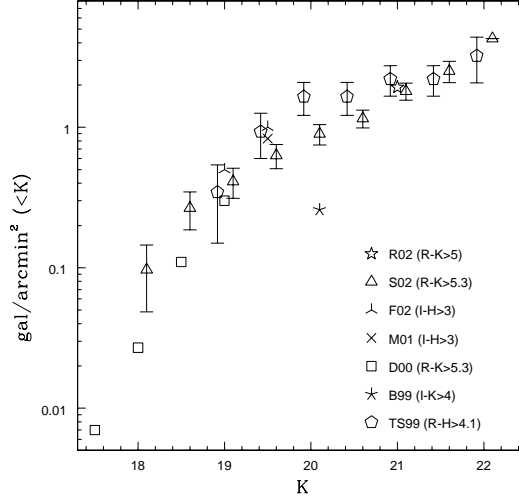


Fig. 1.2. Cumulative number density of Extremely Red Objects for similar color definitions (see references for details; R02=Roche et al. 2002; S02=Smith et al. 2002; F02=Firth et al. 2002; M01=McCarthy et al. 2001; D00=Daddi et al. 2000a; B99=Barger et al. 1999; TS99=Treu & Stiavelli 1999). The outlier B99 is measured from the Hubble Deep Field alone – which is thought to be deficient in high redshift E+S0s. This is a clear example of the effects of cosmic variance and an illustration of the need for a wide field of view and multiple lines of sight.

uncertainties in luminosity evolution. It is clear that in order to perform a reliable comparison with the local LF it is necessary to go significantly fainter than L_* (corresponding to $K=18\text{--}18.5$ adopting the N02 LF and a reasonable range of evolutionary models). It is thus necessary to reach beyond $K=20.5\text{--}21$ to make the uncertainty on $L_*/$ luminosity evolution smaller than the observational errors on the number counts.

The uncertainties related to modeling the star formation history are more dramatic. It is sufficient to have a small amount of recent star formation to make the optical to infrared color significantly bluer and therefore change dramatically $\mathcal{Z}(L)$, and hence the predicted number counts (see discussion in Jimenez et al. 1999). Without more information on the star formation history of E+S0s (see 1.3), it is convenient to adopt the following approach. Models with no delayed star formation (single burst) will predict the maximum density of red E+S0s at high- z . A comparison with these models defines the fraction of local E+S0s already “old” at $z \sim 1$ (Treu & Stiavelli 1999).

How do the EROs counts compare with PLE models? I summarize some of the observational results in Table 1.1 (the deepest and widest for which I could find a PLE comparison). At first glance the results seem highly discrepant. However, some of the fractions in Table 1.1 are with respect to the LF of pure ellipticals (M94 and 0.15K G97; see Fig. 1.1) and not of ellipticals *and* lenticulars. If we assume for simplicity that E and S0 galaxies are present approximately in equal numbers at these luminosities, we have to halve the fractions of McCarthy et al. (2001), Daddi et al. (2000b) and Smith et al. (2002) to obtain the ratio

Obs./Pred.	Model LF	Area (arcmin ²)	depth	Ref
70 %	$0.15 \times K$ (G97)	2200	$H < 21.0$	McCarthy et al. (2001)
100%	E (M94)	701 ^a	$K < 19.2$	Daddi et al. (2000b)
33 %	E+S0 (K01)	81.5	$K < 21.0$	Roche et al. (2002)
100%	E (M94) ^b	49 ^a	$K < 21.6$	Smith et al. (2002)
25 %	$0.32 \times K$ (G97)	13.8 ^a	$H < 23.2$	Treu & Stiavelli (1999)

Table 1.1. *Number density of EROs with respect to the prediction of PLE models.* Column Obs./Pred. lists the fraction of predicted galaxies that is observed, i. e. observed/predicted. Model LF lists the local LF assumed in the PLE models (Notation as in Fig. 1.1). (a) Area is a function of depth; I report here the maximum area and depth (see references for details). (b) PLE models from Daddi et al. (2000b).

Fraction of E+S0	Instrument	Number of EROs	Ref
25-35 %	WFPC2	115	Yan & Thompson (2003)
20-50 %	WFPC2	60	Smith et al. (2002)
50-80 %	NICMOS/WFPC2	41	Moriondo et al. (2000)
55-75 %	NICMOS	30	Stiavelli & Treu (2001)

Table 1.2. *Morphology of EROs. Fraction of EROs with E+S0 morphology found by various surveys at infrared (NICMOS) or optical (WFPC2) wavelengths.*

between the density of EROs and that of local E+S0s (35%, 50%, 50% respectively). The corrected fractions are in much better mutual agreement and range between 25 and 50%. This range can be readily explained in terms of measurement errors, and different star formation histories and local LF adopted in the PLE models. A further correction is required, because we have to take into account the presence of possible contaminants, such as highly dust enshrouded starbursts or reddened AGNs (e.g., Smail et al. 2002). To address this, researchers have relied on HST images, to determine what fraction of EROs are *morphologically* E+S0s. A list of the determinations of morphological fractions among EROs to date is shown in Table 1.2. It is sufficient to multiply the corrected fractions from Table 1.1 by the fractions in Table 1.2 to obtain the density of red E+S0s $z \sim 1$. The density of red E+S0s at $z \sim 1$ is 8%-40% of the local value, with most of the range coming from the uncertainties in Table 1.2. Even allowing for some extra uncertainty related to the range of local LF it seems clear that the number of E+S0s already “old” at $z \sim 1$ is less than in the local universe.

Where are the rest of them? Either they are not yet assembled, or they are simply not recognizable. The latter alternative would be for example the case in a “frosting” (Trager et al. 2000) scenario, where most of the stellar mass is assembled at early-times, while low levels of star formation contribute the rest of the stellar mass at later times. In this scenario, some E+S0s would be too blue at $z \sim 1$ to make it into EROs samples (c.f. the range in rest frame UV colors reported by Moustakas et al. 1997 and McCarthy et al. 2001 for EROs). Star

formation can also alter morphology. For example, if the secondary star formation activity is concentrated in the disk of an S0, the disk would become more prominent and active at $z \sim 1$, transforming the S0 into an Sa. This mechanism, of course, would be effective only on lenticulars and not on pure ellipticals. Therefore it could perhaps provide an explanation of the deficit of “old” spheroids in terms of a demise of lenticulars together with an almost constant number density of ellipticals (similarly to what is seen in clusters; Dressler et al. 1997; Fasano et al. 2000). Deeper, multicolor, high resolution observations are needed to test whether the number density evolution of Es and S0s is different.

Let us now turn our attention to semi-analytic hierarchical models. How do their predictions compare with EROs surface density? Generally, models significantly under-predict the surface density of EROs. For example Firth et al. (2002) and Smith et al. (2002) find 4.5 and 10 times more EROs than expected in the models, a statistically significant disagreement. Again, we face two possible solutions for the disagreement. Either hierarchical models do not produce enough massive systems at $z \sim 1$, or simply their colors are wrong. This latter possibility can occur as a result of an excess of delayed star formation, or as a result of inappropriate treatment of star formation and dust extinction in semi-analytic models.

To summarize, it seems that measurements of the basic observable (EROs surface density; Fig. 1.2) is reaching a reasonable level of mutual agreement. A further improvement would be to gather redshifts for large number of EROs in order to pin down the effective redshift selection functions and the three dimensional space density. Significant efforts are ongoing (Cimatti et al. 2002b; Ellis et al. 2003), and are expected to provide this piece of information soon, at least at the bright end ($K < 19 - 20$). In spite of these achievements, the interpretation of the observations is still open. It seems clear that E+S0s in the local Universe are not all “old” (as in a single burst of star formation at high redshift) and hierarchical models underpredict the density of EROs. It is still disputed whether this discrepancy can be accounted for by improving the treatment of star formation or it is rather pointing to fundamental problems in the *standard model*.

Observations can help addressing this issue in at least two ways. On the one hand they can provide new constraints less critically dependent on star formation history (such as the distribution of redshifts for K-band selected objects described by Kauffmann & Charlot 1998 and Cimatti et al. 2002a; or the mass focused approach described in Section 3). On the other hand, observations can help by providing independent and detailed information on the star formation history of E+S0s.

1.3 Star formation history

We now turn to observational constraints on the star formation history of E+S0s, particularly those obtained from the redshift evolution of the color magnitude relation (1.3.1) and the Fundamental Plane (1.3.2). Where possible, I will discuss both cluster and field observations. Contrasting and connecting the trends across environments is not only crucial to obtain a complete empirical picture, but also to test if the formation of E+S0s is delayed in low density environments as predicted by the *standard model* (Kauffmann 1996).

1.3.1 The colors of distant E+S0 galaxies

In the local Universe E+S0s obey a color-magnitude relation (CMR): brighter E+S0s are redder than less luminous ones. At a given absolute magnitude, the scatter in optical and infrared colors – at least in clusters – is minimal (< 0.05 mags; Bower, Lucey & Ellis 1992).

T. Treu

The widely accepted interpretation is that brighter E+S0s are more metal rich and that star formation in cluster E+S0s happened and ceased early enough in cosmic time that the effects of possible spread in formation epoch are non detectable through broad band colors (see Bower, Kodama & Terlevich 1998 for caveats). The most convincing evidence in support of this interpretation is the redshift evolution of the CMR. The almost constant slope of the color-magnitude relation with redshift shows directly that it is not an age-mass sequence (Ellis et al. 1997; Kodama et al. 1998). Similarly, the small scatter found in high-z clusters indicates that the stellar populations of massive cluster E+S0s are uniformly old ($z_f > 2$) and quiescent (Stanford, Eisenhardt & Dickinson 1995, 1998; Ellis et al. 1997), with the possible exception of S0s at large cluster radii (van Dokkum et al. 1998b). What prevents this from being a simple and well defined picture is that E+S0s in high redshift clusters are not the only possible progenitors of present day cluster E+S0. Some of the progenitors at $z \sim 1$ might not have yet been accreted onto the cluster, or might not be morphologically recognizable. Therefore, the tightness of the CMR in high-z clusters could in part be due to a selection effect (“progenitor bias”; van Dokkum & Franx 2001). However, the observed evolution of the morphology-density relation (Dressler et al. 1997; van Dokkum et al. 2001; Treu et al. 2003) can be used to quantify the bias and rules out the most dramatic scenarios.

Less well studied is the CMR in the general field. The few studies available seem to indicate that there is a CMR in the field out to $z \sim 1$, although with considerably more scatter than in clusters (Franceschini et al. 1998; Kodama, Bower & Bell 1999; Schade et al. 1999). Similarly, the Hubble Deep Fields show strong variations in internal color, often associated with blue cores (Menanteau, Abraham & Ellis 2001), at variance with the homogeneous population and red color gradients (Saglia et al. 2000) observed in clusters at similar redshifts.

1.3.2 *The Fundamental Plane of distant E+S0 galaxies*

Can we now measure the star formation history of E+S0s at a given mass? A promising way to do this is by studying the evolution with redshift of the Fundamental Plane (Djorgovski & Davis 1987; Dressler et al. 1987; Jørgensen, Franx & Kjærgaard 1996; hereafter FP). The FP is a tight empirical correlation between the effective radius R_e , velocity dispersion σ , and effective surface brightness SB_e , of equation:

$$\log R_e = \alpha \log \sigma + \beta SB_e + \gamma, \quad (1.2)$$

where α and β are called the slopes, while γ is called the intercept. The very existence of the FP is a remarkable fact. Any theory of galaxy formation and evolution must be able to account for its tightness (0.08 rms in $\log R_e$). For discussion of possible physical explanations of the FP relation see references in Treu et al. (2001).

Independent of its origin, the evolution of the FP with redshift can be linked to the evolution of the stellar mass-to-light ratio of E+S0s, and hence of their star formation history, in the following way. Let us define an effective mass $M \equiv \sigma^2 R_e$. If homology holds, i.e. early-type galaxies are structurally similar, the total mass \mathcal{M} (including dark matter if present) is proportional to M and the effective mass can be interpreted in terms of the Virial Theorem (e.g. Bertin, Ciotti & del Principe 2002). Similarly, an effective luminosity can be defined as $\log L = -0.4SB_e + 2\log R_e + \log 2\pi$. Based on these definitions, the M/L (effective mass-to-light ratio) of a galaxy is readily obtained in terms of

T. Treu

the FP observables: $M/L \propto 10^{0.4SB_e} \sigma^2 R_e^{-1}$. Using the FP relation to eliminate SB_e yields $M/L \propto 10^{-\frac{\gamma}{2.5}} \sigma^{\frac{10\beta-2\alpha}{5\beta}} R_e^{\frac{2-5\beta}{5\beta}}$

Consider a sample of galaxies at $z > 0$ identified by a running index i . The offset of M/L from the local value can be computed as

$$\Delta \log(M/L)^i = \Delta \left(\frac{10\beta-2\alpha}{5\beta} \right) \log \sigma^i + \Delta \left(\frac{2-5\beta}{5\beta} \right) \log R_e^i - \Delta \left(\frac{\gamma^i}{2.5\beta} \right), \quad (1.3)$$

where the symbol Δ indicates the difference of the quantity at two redshifts, and γ^i is defined as $\log R_e^i - \alpha \log \sigma^i - \beta SB_e^i$. For the analysis presented here I will assume that α and β are constant (see Treu et al. 2001 for discussion). This assumption is consistent with the observations and makes the interpretation of the results straightforward. If α and β are constant – and there is no structural evolution (so that R_e and σ are constant) – then $\Delta \log(M/L^i) = -\frac{\Delta \gamma^i}{2.5\beta}$, i.e. the evolution of $\log(M/L^i)$ depends only on the evolution of γ^i . Measuring γ^i for a sample of galaxies at intermediate redshift, and comparing it to the value of the intercept found in the local Universe, measures the average evolution of $\log(M/L)$ with cosmic time as $\langle \Delta \log(M/L) \rangle = -\frac{\langle \Delta \gamma \rangle}{2.5\beta}$. If the evolution of the effective mass-to-light ratio measures the evolution of the stellar mass-to-light ratio, then the FP becomes a powerful diagnostic of stellar populations. Not only this diagnostic connects stellar populations to a dynamical mass measurement, but it is also intrinsically tight, and thus selection effects are small and can be corrected (Treu et al. 2001; Bernardi et al. 2003).

Several groups have applied this technique at $z > 0.1$, both in clusters (Franx 1993; van Dokkum & Franx 1996; Kelson et al. 1997; Bender et al. 1998; van Dokkum et al. 1998a; Jørgensen et al. 1999; Kelson et al. 2000; Ziegler et al. 2001; van Dokkum & Stanford 2003; Fritz et al. 2003), and in the field (Treu et al. 1999; 2001a,b, 2002; van Dokkum et al. 2001; Bernardi et al. 2003). A representative selection of results is shown in Figure 1.3. The main results of these studies are: 1) E+S0s obey a FP relation out to at least $z \sim 0.8$ with scatter similar to local samples (in the field the scatter in $\log R$ is less than 0.15 at $z \sim 0.8$; Treu et al. 2002); 2) field E+S0s (solid pentagons) evolve faster than cluster ones (open squares). In quantitative terms, Treu et al. (2002) obtain $d(\log M_*/L_B)/dz = -0.72_{-0.16}^{+0.11}$ for the field sample, while van Dokkum et al. (1998a) obtain -0.49 ± 0.05 for clusters. Note the good agreement with the results obtained by I02 from the evolution of the LF (1.2.1).

In terms of evolution of stellar populations, the cluster data are consistent with passive evolution of an old stellar population ($z_f \sim 2$). A more recent “epoch of formation” $z_f \sim 1.3$ appears to be needed to explain the field E+S0s evolution in terms of single burst stellar populations. However, as for the EROs PLE models, it is sufficient to rejuvenate an old stellar population with a small amount of recent star formation to obtain an evolution consistent with the data. For example, the data are well described by a model where 90% of the stellar mass is formed at $z_{f1} \sim 2$ and secondary bursts at $z_{f2} \sim 1$ contribute the residual 10 %.

1.3.3 Discussion

Both the evolution of colors and FP to $z \sim 1$ appear to be consistent with the following picture. Massive cluster E+S0s are old and quiescent, while field examples show some relatively recent star formation activity. This picture is also in qualitative agreement with the fact that *at any given morphological type* star formation activity decreases monotonically with (local) galaxy density (see, e.g. Poggianti et al. 1999; Poggianti, Dressler & Nichol,

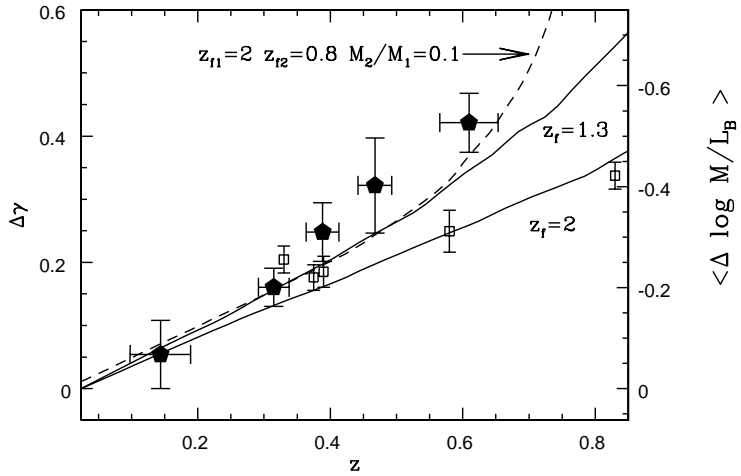


Fig. 1.3. FP in the rest-frame B band. The average offset of the intercept of field galaxies (Treu et al. 2002) from the local FP relation as a function of redshift (large filled pentagons) is compared to the offset observed in clusters (open squares; van Dokkum & Franx 1996; Kelson et al. 1997; Bender et al. 1998; van Dokkum et al. 1998a; Kelson et al. 2000). The solid lines represent the evolution predicted for passively evolving stellar populations formed in a single burst at $z = 1.3, 2$ (from top to bottom) computed using Bruzual & Charlot (1993) models in the BC96 version. The evolution predicted by a double-burst model is also shown for comparison. See Treu et al. (2002) for details.

these proceedings), and observations of high redshift E+S0s based on other spectroscopic diagnostic features (Schade et al. 1999; Kelson et al. 2001; Treu et al. 2002). Further support for this picture comes from the fossil evidence (Bernardi et al. 1998; Trager et al. 2000; Kuntschner et al. 2002), although interpreting the observations in the local Universe is more difficult, because possible differences could have been quenched by time to a level where uncertainties on dust extinction and absolute distances (Pahre, Djorgovski & de Carvalho 1998), and the age/metallicity degeneracy (Kuntschner et al. 2002) are significant.

How does this picture compare with CDM predictions? *Qualitatively*, the observational picture is similar to theoretical predictions (Diaferio et al. 2001; Benson et al. 2002). However, *quantitatively*, the observed differences between the star formation history of field and cluster E+S0s are smaller than predicted by models. Whereas observations indicate at most minor departures from a single old stellar populations, hierarchical models predict dramatic differences already at $z < 0.5$ (see Kauffmann 1996 and van Dokkum et al. 2001). As it was the case for EROs, improvements in the treatment of star formation or of environmental effects might reconcile the model with the data. Alternatively, this might prove a major problem for the *standard model*, especially when more precise measurements will be available. From an observational point of view, it has to be noticed that current studies are based on few tens of objects at most. It is now crucial to collect high quality data on larger numbers of distant E+S0s to overcome small sample statistics and cosmic variance.

1.4 The mass density profile of distant E+S0 galaxies

So far, in this review, I have interpreted observations in terms of pure luminosity evolution. For example, when expressing the evolution of the FP in terms of evolution of stellar mass-to-light ratio, I have assumed pure luminosity evolution. Is there any way we can relax this assumption and measure directly and simultaneously the internal structure and stellar populations properties of distant E+S0s? If we could, not only we could test if the results obtained under a pure luminosity evolution hypothesis are correct, but also, and most importantly, we could gain new and fundamentally different insight into the evolution of E+S0s. For example, measuring the mass density profile of luminous and dark matter in E+S0s as a function of redshift not only yields an independent determination of the evolution of the stellar mass to light ratio, but also tests the existence of the universal dark matter profile predicted by the *standard model*. Furthermore, theoretical predictions related to the mass density profile and orbital structure might not be as dramatically sensitive to the details of the treatment of star formation as, e.g., EROs number density. Therefore, testing these predictions might be a more robust way to test the *standard model*.

Measuring the mass density profile of E+S0s is already challenging in the local Universe (e.g. Bertin et al. 1994), and traditional methods are inapplicable at high redshift (for example surface brightness dimming prevents the measurement of very extended velocity dispersion profiles). Nevertheless, mass density profile measurements at high redshifts are possible because distant E+S0s are efficient gravitational lenses. The next two sections describe recent results on the mass density profile of distant E+S0s from weak lensing (1.4.1), and joint strong lensing and dynamical analysis (1.4.2).

1.4.1 Galaxy-galaxy lensing

The distortion of background galaxies lensed by an individual E+S0s is not detectable. However, if several (at least hundreds) E+S0s are considered, and the signal from all the background objects is coadded, a statistical measurement of mass density profile of the average galaxy can be derived (Brainerd, Blandford & Smail 1996). This technique is known as galaxy-galaxy lensing and has proved viable to study the outer regions of the dark matter halos of E+S0s (Griffiths et al. 1996). For example, dark matter halos around red galaxies have been detected out to several hundreds kpc in SDSS images (McKay et al. 2003). Combining information from galaxy-galaxy lensing with the existence of the FP, Seljak (2002) showed that at large radii the mass density profile of E+S0s declines faster than r^{-2} , consistent with the r^{-3} behavior predicted by CDM numerical simulations. Natarajan & Kneib (1997) and Natarajan et al. (1998) showed that dark matter halos of E+S0s can be detected even within clusters if the cluster potential is appropriately modeled. Natarajan, Kneib & Smail (2002) applied this technique to WFPC2 images of a sample of intermediate redshift clusters, and showed that dark matter halos of E+S0s are truncated as expected from tidal interaction with the cluster.

1.4.2 Strong lensing and the Lenses Structure and Dynamics Survey

The majority of the almost hundred galaxian gravitational lenses known are E+S0s. Once the redshift of the lens and the source are known, the geometry of the multiple images provides a very robust measurement of the mass enclosed by the Einstein Radius R_E . The Einstein Radius of the typical $z \sim 0.5$ E+S0s lens galaxy is larger than the effective radius.

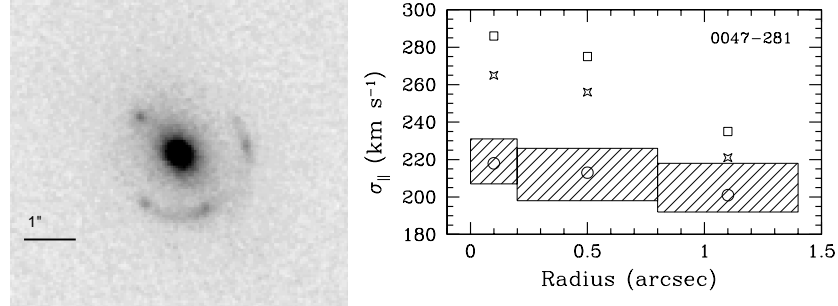


Fig. 1.4. Left: HST image of 0047–281 at $z = 0.485$. Right: velocity dispersion profile of 0047–281 along the major axis. The box height indicates the 68% measurement error, whereas the box width indicates the spectroscopic aperture. The open squares are the corresponding values for an isotropic constant M/L model, which is rejected by the data. See Koopmans & Treu (2003) for details.

Thus strong lensing can be used to determine total mass at large radii for tens of distant E+S0s, independent of the nature and dynamical state of the mass inside R_E .

In some cases, knowledge of the mass enclosed by R_E is already sufficient to show that the average total mass-to-light ratio is larger than expected for reasonable stellar populations, and therefore to prove the existence of dark matter. Unfortunately, not much information is generally provided on how mass is spatially distributed[§].

Nevertheless, assuming a mass density profile, lensing can be used to probe the evolution of the stellar populations. For example, Kochanek et al. (2000) and Rusin et al. (2003) used image separation to estimate the velocity dispersion of lens E+S0s assuming a singular isothermal total mass density profile (i.e. the total density $\rho_t \propto r^{-2}$). With this assumption they measure the evolution of the FP of lens galaxies and find $d(\log M_*/L_B)/dz = -0.54 \pm 0.09$, i.e. more similar to the cluster value than the field value (a similar analysis of lens E+S0s by van de Ven et al. (2003), yields -0.62 ± 0.13). The marginally significant differences with respect to the direct method could be the result of different selection processes (lenses are “mass” selected, while samples used in direct measurements are “light” selected), of different environments (lenses might be preferentially found in groups or small clusters; Fassnacht & Lubin 2002), or of external contributions to the image separation (such as from a nearby group or cluster). Or perhaps, the differences could be an indication of small departures from isothermal mass density profiles. However, the ability of a simple singular isothermal mass model to predict with reasonable accuracy the central velocity dispersion is remarkable (as generally confirmed by direct measurement, e.g., Koopmans & Treu 2002). This is an indication of the overall structural homogeneity of E+S0s. The accuracy of the predicted σ is even more remarkable considering that $R_E/R_e \sim 0.5–5$, and therefore lensing probes regions dominated by stellar mass as well as regions dominated by dark matter.

More can be learned on the internal mass distribution of distant E+S0s by combining strong lensing constraints with spatially resolved stellar kinematics of the lens galaxy, in a joint lensing and dynamical analysis. The two diagnostics complement each other reducing

[§] Except perhaps when the lensed source is extended and the detailed geometry can be used to increase the number of constraints (see, e. g., Blandford et al. 2001; Kochanek et al. 2001; Saha & Williams 2001)

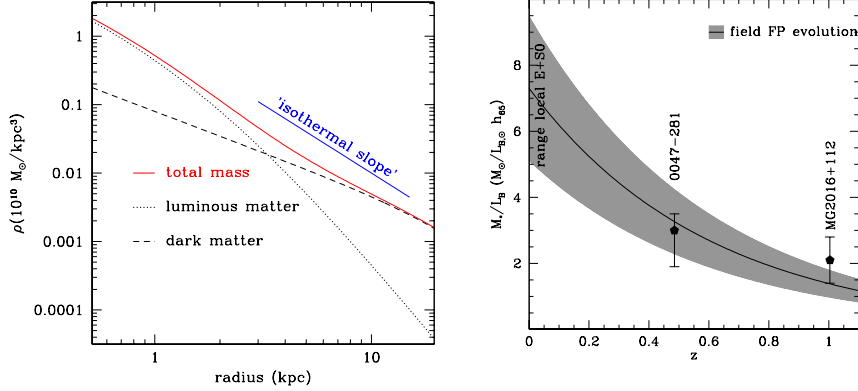


Fig. 1.5. Left: best fitting mass model of MG2016+112 at $z=1$ (see Treu & Koopmans 2002a for details). Right: comparison between the evolution of stellar the mass to light ratio measured via the FP evolution and via a joint lensing and dynamical analysis by the LSD Survey (see text for detail).

the degeneracies inherent to each method. Stellar kinematics constrains the mass distribution within the Einstein radius, while gravitational lensing analysis fixes the mass at the Einstein radius, thus lifting the so-called mass-anisotropy degeneracy (Treu & Koopmans 2002, Koopmans & Treu 2003).

Combining the two diagnostics is the goal of the Lenses Structure and Dynamics Survey (Koopmans & Treu 2002, 2003; Treu & Koopmans 2002a, b; hereafter collectively KT). In eight clear nights at the Keck-II Telescope we have collected data to measure accurate and spatially resolved stellar kinematics for a sample of 11 gravitational lenses out to $z \sim 1$ with available HST images. An example of the data is shown in Figure 1.4.

A family of two-component spherical mass models is used in the joint lensing and dynamical analysis (see KT for details). One component is the stellar component, assumed to follow the surface brightness profile as measured from HST images scaled by a constant stellar mass to light ratio (M_*/L_B). The other component is the dark matter halo, modeled as a generalized NFW profile, where the dark matter density goes as r^{-3} at large radii and $r^{-\gamma}$ at small radii. Comparison with the data yields best fitting models and likelihood contours on the relevant parameters (M_*/L_B and γ).

The best fitting mass model for MG2016+112 at $z=1.004$ (Lawrence et al. 1984) is shown in the left panel of Fig. 1.5. Luminous mass dominates in the inner ~ 10 kpc while a flatter dark matter halo contributes most of the mass at larger radii. No dark matter models, or constant total mass-to-light ratio models, are rejected at high confidence level. Remarkably, although none of the two components is a simple power law density profile, the *total* mass density profile follows very closely an r^{-2} singular ‘‘isothermal’’ profile (equivalent to a flat rotation curve for spiral galaxies). The same result is recovered by modeling the lens with a simple power law mass density profile $\rho_t \propto r^{-\gamma'}$. Comparison with the data yields $\gamma = 2.0 \pm 0.1 \pm 0.1$. Similar results are found for the other object analyzed so far, 0047-281 (Warren et al. 1996) at $z=0.485$. There is strong evidence for a dark matter halo more

diffused than the luminous component and the total mass density profile is close to a singular isothermal profile, well described by a power law with effective slope $\gamma' = 1.90^{+0.05}_{-0.23} \pm 0.1$.

The joint lensing and dynamical analysis also yields a measurement of M_*/L_B , which can be used to measure the evolution of stellar population independently of the FP analysis (1.3.2). In the right panel of Fig. 1.5 the LSD results are compared with the FP results. Since the FP analysis only yields $d(\log M_*/L_B)/dz$, I adopted for the comparison the 7.8 ± 2.7 in solar units for the range of local values (KT). The agreement is very good, consistent with the expectations of a pure luminosity evolution scenario.

Finally, observational limits on γ can be used to test the cuspy dark matter halos predicted by CDM scenarios ($\gamma = 1$ NFW; $\gamma = 1.5$ Moore et al. 1998). For the first two objects we find upper limits $\gamma < 1.4$ and $\gamma < 1.5$ (68% CL) consistent with the results of numerical simulations only if the collapse of baryons to form stars (which dominates in the inner regions) did not steepen significantly the dark matter halos. The analysis of the complete sample will hopefully provide more stringent limits.

Although the results so far have to be considered preliminary since they are based on the first two objects, three facts appear to stand out: i) E+S0s at high redshift have diffuse dark matter halos; ii) luminous and dark matter, although spatially segregated, “conspire” to follow an almost isothermal total mass density profile, similarly to what happens in local E+S0 and spiral galaxies (van Albada & Sancisi 1986; Rix et al. 1997); iii) the agreement between the evolution of the mass to light ratio measured by the FP and the direct measurements is consistent with no structural evolution of E+S0s in the past 8 Gyrs.

The first point, direct evidence of extended dark matter halos around E+S0s out to $z \sim 1$, is probably not surprising, but it is a confirmation of the CDM scenario. The second point, the “conspiracy” between luminous and dark matter to produce r^{-2} – that appears to be a consistent feature of early-type and spiral galaxies out to $z \sim 1$ – is something that should be explained by a satisfactory cosmological model. It is not clear if this is the case in the *standard model*, since simulations do not generally include baryons. Analytic approximations of baryonic collapse (Blumenthal et al. 1986) do not explain naturally this result. An alternate explanation might be that the r^{-2} profile, the limit of (incomplete) violent relaxation (Lynden-Bell 1967), is a *dynamical attractor*. If baryons are transformed in stars early enough (as in the monolithic collapse scenario by van Albada 1982 or as recently proposed by Loeb & Peebles 2003), then they behave as dissipationless particles and could interact with dark matter so as to tend to a *total* mass density profile that is close to the dynamical attractor (Loeb & Peebles 2003), while preserving spatial segregation as a result of different initial conditions. Finally, the third point, the lack of dynamical evolution out to $z \sim 1$, together with other evidence for homogeneity of E+S0s described in the previous sections, appears to be another challenge for the *standard model*. If E+S0s are formed by mergers, then either mergers have to occur very early in cosmic time, or some sort of fine tuning of the merging process appears to be required in order to produce such homogeneous end-products.

1.5 Acknowledgments

I am grateful to Giuseppe Bertin and Richard Ellis for their comments on an earlier version of this manuscript, and to my collaborators Stefano Casertano, Léon Koopmans, Palle Møller, and Massimo Stiavelli for innumerable stimulating discussions. I acknowledge useful conversations with Masataka Fukugita, Myungshin Im, Pat McCarthy, Alvio Renzini,

T. Treu

David Sand, Graham Smith. I would like to thank the organizers for this exciting meeting, and the referee, Alan Dressler, for insightful comments.

References

- Barger A. J., Cowie L. L., Trentham N., Fulton E., Hu E. M., Songaila A., & Hall D., 1999, AJ, 117, 102
Bender, R., Saglia, R. P., Ziegler, B., Belloni, P., Greggio, L., Hopp, U., & Bruzual, G., 1998, ApJ, 493, 529
Benitez N., Broadhurst T., Bouwens R., Silk J., & Rosati P., 1999, ApJ, 515, L65
Benson, A. J., Ellis, R. S. & Menanteau, F. 2002, MNRAS, 336, 564
Bernardi, M., Renzini, A., da Costa, L. N., Wegner, G., Alons, M. V., Pellegrini, P.S., Rite, C., & Willmer, C.N.A. 1998, ApJ, 508, L143
Bernardi, M., et al. 2003, AJ, 125, 1866
Bertin, G., & Stiavelli, M., 1993, Rep. Prog. Phys., 56, 493
Bertin, G., Ciotti, L., & del Principe M. 2002, A&A, 386, 149
Bertin, G., et al. 1994, A&A, 292, 381
Blandford, R.D., Surpi, G., & Kundic, T. 2001, in “Gravitational Lensing: Recent Progress and Future Goals”, ASP. Vol. 237. Brainerd, T. G., & Kochanek C. S. eds.
Blumenthal, G. R., Faber, S. M., Flores, R., & Primack, J. R. 1986, ApJ, 301, 27
Blumenthal, G. R., Faber, S. M., Primack, J. R., & Rees, M. J., 1984, Nature, 311, 517
Bower, R. G., Lucey, J. R., & Ellis, R. S. 1992, MNRAS, 254, 601
Bower, R.G., Kodama, T., & Terlevich, A. 1998, MNRAS, 299, 1193
Brainerd, T. G., Blandford, R. D., & Smail, I. 1996, ApJ, 466, 6 23
Bruzual, G.A. , & Charlot, S. 1993, ApJ, 405, 538
Chen, H.-W., et al. 2002, ApJ, 570, 54
Cimatti, A., et al. 2002a, A&A, 391, L1
———. 2002b, A&A, 392, 395
Cohen, J.G. 2002, ApJ, 567, 672
Corbin, M.R., O’Neil, E., Thompson, R.I., Rieke, M.J., & Schneider, G. 2000, AJ, 120, 1209
Daddi, E., Cimatti, A., Pozzetti, L., Hoekstra, H., Röttgering, H.J.A., Renzini, A., Zamorani, G., & Mannucci, F. 2000a, A&A, 361, 535
Daddi, E., Cimatti, A., & Renzini, A. 2000b, A&A, 362, L45
de Freitas Pacheco, J. A., Michard, R., & Mohayaee R. 2003, preprint, astro-ph/0301248
de Vaucouleurs G., 1948, Ann. Astrophys., 11, 247
de Zeeuw, T., & Franx, M., 1991, ARA&A, 29, 239
Diaferio, A., Kauffmann, G., Balogh, M., White, S.D.M., Schade, D., & Ellingson, E. 2001, MNRAS, 323, 999
Djorgovski, S. G., & Davis, M. 1987, ApJ, 313, 59
Dressler, A., Lynden-Bell, D., Burstein, D., Davies, R. L., Faber, S. M., Terlevich, R., & Wegner G. 1987, ApJ, 313, 42
Dressler, A., et al. 1997, ApJ, 490, 577
Eggen, O.J., Lynden-Bell, D., & Sandage A. 1962, ApJ, 136, 748
Ellis R. S., Smail I., Dressler A., Couch W. J., Oemler A., Butcher H., & Sharples R. M., 1997, ApJ, 483, 582
Ellis, R.S., et al. 2003, in preparation
Fasano, G., Poggianti, B.M., Couch, W.J., Bettoni, D., Kjærgaard, P., & Moles, M. 2000, ApJ, 542, 673
Fassnacht, C. D., & Lubin, L. L. 2002, AJ, 123, 627
Firth, A. E., et al. 2002, MNRAS, 332, 617
Franceschini A., Silva L., Fasano G., Granato L., Bressan A., Arnouts S., & Danese L., 1998, ApJ, 506, 600
Franx, M. 1993, ApJ, 407, L5
Fritz, A. 2003, Carnegie Observatories Astrophysics Series, Vol. 3: Clusters of Galaxies: Probes of Cosmological Structure and Galaxy Evolution, ed. J. S. Mulchaey, A. Dressler, and A. Oemler (Pasadena: Carnegie Observatories, <http://www.ociw.edu/ociw/symposia/series/symposium3/proceedings.html>)
Fukugita, M., Shimasaku, K., & Ichikawa, T. 1995, PASP, 107, 945
Gardner, J. P., Sharples, R.M., Frenk, C.S., & Carrasco, B.E. 1997, ApJ, 480, L99
Griffiths, R. E., Casertano, S., Im, M., & Ratnatunga, K. 1996, MNRAS, 281, 1159
Im, M., Faber, S. M., Koo, D. C., Phillips, A. C., Schiavon, R. P., Simard, L., & Willmer, C. N. A., 2002, ApJ, 571, 136

T. Treu

- Im, M., Griffiths, R. E., Ratnatunga, K. U., & Sarajedini, V. L. 1996, ApJ, 461, 79
Jimenez R., Friaca A. C. S., Dunlop J. S., Terlevich R. J., Peacock J. A., & Nolan L. A., 1999, MNRAS, 305, L16
Jørgensen, I., Franx, M., Hjorth, J., & van Dokkum, P. G., MNRAS, 1999, 308, 833
Jørgensen, I., Franx, M., & Kjærgaard, P. 1996, MNRAS, 280, 167
Kauffmann, G. 1996, MNRAS, 281, 487
Kauffmann, G., & Charlot 1998, MNRAS, 297, L23
Kauffmann, G., & Haehnelt M. G. 2000, MNRAS, 311, 576
Kelson D. D., Illingworth G. D., van Dokkum, P. G., & Franx, M. 2000, ApJ, 531, 184
Kelson, D. D., van Dokkum, P. G., Franx, M., Illingworth G. D., & Fabricant, D. G. 1997, ApJ, 478, L13
Kodama, T., Arimoto, N., Barger, A. J., & Arag'on-Salamanca, A. 1998, A&A, 334, 99
Kodama, T., Bower, R. G., & Bell, E. F. 1999, MNRAS, 306, 561
Kochanek, C. S., et al. 2000, ApJ, 543, 131
Kochanek, C. S., Keeton, C.R., & McLeod, B. 2001, ApJ, 547, 50
Kochanek, C. S., et al. 2001, ApJ, 560, 666
Koopmans, L. V. E., & Treu, T., 2002, ApJ, 568, L5
———. 2003, ApJ, 583, 606
Kuntschner, H., Smith, R.J., Colless, M., Davies, R.L., Kaldare, R., & Vazdekis, A. 2002, MNRAS, 337, 172
Larson, R. B. 1975, MNRAS, 173, 671
Lawrence, C.R., Schneider, D. P., Schmidet, M., Bennett, C. L., Hewitt, J. N., Burke, B. F., Turner, E. L., & Gunn, J. E. 1984, Sci, 223, 46
Lynden-Bell, D. 1967, MNRAS, 136, 101
Loeb, A., & Peebles, P. J.E. 2003, ApJ, 589, L29
Marinoni, C., Monaco, P., Giuricin, G., & Costantini, B. 1999, ApJ, 521, 50
Martini, P. 2001, AJ, 121, 598
Marzke, R., Geller, M. J., Huchra, J. P., & Corwin, H.G. 1994, AJ, 108, 437
Marzke, R., da Costa, L. N., Pellegrini, P. S., Willmer, C. N. A., & Geller, M. J. 1998, ApJ, 503, 617
Matteucci, F. 2002, preprint, astro-ph/0210540
McCarthy, P., et al. 2001, ApJ, 560, L131
McCracken, H. J., Metcalfe, N., Shanks, T., Campos, A., Gardner, J. P., & Fong, R. 2000, MNRAS, 311, 707
McKay, T., et al. 2003, ApJ, submitted, astro-ph/0108013
Menanteau, F., Abraham, R. G., & Ellis, R. S. 2001, MNRAS, 322, 1
Menanteau F., Ellis R. S., Abraham R. G., Barger A.J., & Cowie L. L., 1999, MNRAS, 309, 208
Merritt, D., 1999, PASP, 111, 129
Meza, A., Navarro, J., Steinmetz, M., & Eke, V. R., ApJ, submitted, astro-ph/0301224
Moore, B., Governato, F., Quinn, T., Stadel, J., & Lake, G., 1998, ApJ, 499, L5
Monaco, P., Salucci, P., & Danese L, 2000, MNRAS, 311, 279
Moriondo, G., Cimatti, A., & Daddi, E. 2000, A&A, 364, 26
Moustakas, L. A., Davis, M., Graham, J. R., Silk, J., Peterson, B.A., & Yoshii, Y. 1997, ApJ, 475, 445
Nakamura, O., Fukugita, M., Yasuda, N., Loveday, N., Brinkmann, J., Schneider, D. P., Shimasaku, K., & Subbarao, M. 2003, AJ, 125, 1682
Natarajan, P., & Kneib, J.-P. 1997, MNRAS, 287, 833
Natarajan, P., Kneib, J.-P., Smail, I., & Ellis, R.S. 1998, ApJ, 499, 600
Natarajan, P., Kneib, J.-P., & Smail, I. 2002, ApJ, 580, L11
Navarro, J., Frenk, C. S., & White S. D. M., 1997, ApJ, 490, 493
Pahre M. A., Djorgovski S. G., & De Carvalho R. R. 1998b, AJ, 116, 1591
Peebles, P. J. E 2002, preprint, astro-ph/0201015
Poggianti, B., Smail, I., Dressler, A., Couch, W.J., Barger A., Butcher, H., Ellis, R.S., & Oemler, A. 1999, ApJ, 518, 576
Rix, H. W., de Zeeuw, P. T, Cretton, N., van der Marel, R. P., & Carollo, C. M. 1997, ApJ, 488, 702
Roche, N. D., Almaini, O., Dunlop, J., Ivison, R. J., & Willott, C. J. 2002, MNRAS, 337, 128
Rusin, D., et al. 2003, ApJ, 587, 143
Saglia, R.P., Maraston, C., Gregg, L., Bender, R., & Ziegler, B. 2000, A&A, 360, 911
Saha, P., & Williams, L. L. 2001, AJ, 122 585
Sandage, A. 1972, 176, 21
Sandage, A., & Visvanathan, N., 1978, ApJ, 225, 742
Schade, D., et al., 1999, ApJ, 525, 31
Schechter, P. 1976, ApJ, 203, 297

T. Treu

- Seljak, U. 2002, MNRAS, 334, 797
Smith, G.P., et al. 2002, MNRAS, 330, 1
Smail, I., Owen, F. N., Morrison, G. E., Keel, W. C., Ivison, R. J., & Ledlow, M. J., 2002, ApJ, 581, 844
Stanford, S.A., Eisenhardt, P. R., & Dickinson, M. 1995, ApJ, 450, 512
Stanford, S.A., Eisenhardt, P. R., & Dickinson, M. 1998, ApJ, 492, 461
Stiavelli, M., & Treu, T. 2001, in "Galaxy Disks and Disk Galaxies", ASP, vol. 230, Funes S.J. & Corsini E.M.
Thompson, D., et al. 1999, ApJ, 523, 100
Toomre, A., & Toomre, J. 1972, ApJ, 178, 623
Toomre, A. 1977, ARA&A, 15, 437
Trager, S.C. 2003, to appear in Carnegie Observatories Astrophysics Series, vol. 4: Origin and Evolution of the Elements, ed. A. McWilliam & M. Rauch (Cambridge: Cambridge University Press), astro-ph/0307069
Trager, S.C., Faber, S.M., Worthey, G., & Gonzalez, J.J. 2000, AJ, 120, 165
Treu, T., & Koopmans, L.V.E. 2002a, ApJ, 575, 87
———. 2002b, MNRAS, 337, L6
Treu, T., & Stiavelli, M. 1999, ApJ, 524, L27
Treu, T., Ellis, R.S., Kneib, J.-P., Dressler, A., Smail, I., Czoske, O., Oemler, A., & Natarajan, P. 2003, ApJ, 591, 53
Treu, T., Stiavelli, M., Bertin G., Casertano, C., & Møller, P. 2001a, MNRAS, 326, 237
Treu, T., Stiavelli, M., Casertano, C., Møller, P., & Bertin G. 1999, MNRAS, 308, 1037
———. 2002, ApJ, 564, L13
Treu, T., Stiavelli, M., Møller, P., Casertano, S., & Bertin, G. 2001b, MNRAS, 326, 221
van Albada, T. S. 1982, MNRAS, 201, 939
van Albada, T. S. & Sancisi, R. 1986, RSPTA, 320, 447
van de Ven, G., van Dokkum, P.G., & Franx, M. 2003, preprint, astro-ph/0211566
van Dokkum P. G., & Franx M., 1996, MNRAS, 281, 985
———. 2001, ApJ, 553, 90
van Dokkum, P. G., & Stanford, S.A. 2003, ApJ, 562, L35
van Dokkum, P. G., Franx, M., Kelson D. D., & Illingworth G. D., 1998a, ApJ, 504, L17
van Dokkum, P. G., Franx, M., Kelson D. D., & Illingworth G. D., Fisher, D., Fabricant, D., 1998b, ApJ, 504, 714
van Dokkum, P. G., Franx, M., Kelson D. D., & Illingworth G. D., 2001, ApJ, 553, L39
van Dokkum, P. G., Stanford, S.A., Holden, B.P., Eisenhardt, P.R., Dickinson, M.E., & Elston, R. 2001, ApJ, 552, L101
Volonteri, M., Haardt, F., & Madau, P. 2003, 582, 559
Warren, S. J., Hewett, P. C., Lewis, G. F., Møller, P., Iovino, A., & Shaver P. A., 1996, MNRAS, 278, 139
White, S. D. M., & Rees, M. J., 1978, MNRAS, 183, 341
Willis, J. P., Hewett, P. C., Warren, S. J., & Lewis, G. F. 2002, MNRAS, 337, 953
Yan, L., McCarthy, P. J., Weymann, R. J., Malkan, M. A., Teplitz, H. I., Storrie-Lombardi, L. J., Smith, M., & Dressler, A. 2000, AJ, 120, 575
Yan, L., & Thompson, D. 2003, ApJ, 586, 765
Zepf, S. E. 1997, Nature, 390, 377
Ziegler, B. L., Bower, R. G., Smail, I. R., Davies, R. L., & Lee D., 2001, MNRAS, 325, 1571